Kullback-Leibler Divergence Analysis for Integrated Radar and Communications (RadCom)

Mohammad Al-Jarrah, *Member, IEEE*, Emad Alsusa, *Senior Member, IEEE,* and Christos Masouros, *Senior Member, IEEE,*

***Abstract*— In this paper, we provide performance analysis for an integrated radar-communication (RadCom) system based on the relative information (RE), also called the Kullback-Leibler divergence (KLD) theorem. The considered system model consists of a multiple-input-multiple-output (MIMO) base-station (BS) which aims at providing RadCom services to multiple communication user equipments (UEs) and detecting a target. The separated deployment, in which the base-station antennas are distributed among radar and communication subsystems, is considered with Zero forcing (ZF) and maximum ratio transmission (MRT) precoders are applied to precode the communication signal. Results show that the derived formulas in this paper are accurate and imply that MRT suffers from bad performance compared to ZF.**

***Index Terms*— Integrated sensing and communication (ISAC), integrated RadCom system, relative information, Kullback-Leibler distance, zero forcing (ZF), maximum ratio transmission (MRT).**

I. INTRODUCTION

The collection of measurements from the environment about a certain phenomenon can be seen in a massive number of every day applications, such as radar, LiDAR, and IoT applications [1], [2]. In recent types of radars, multiple antennas are employed to transmit/receive the electromagnetic waves. In such types of multiple-input-multiple-output (MIMO) radars, the separation between adjacent antennas is $d \geq \lambda/2$, where d is the antenna separation and λ is the wavelength. With this setup, spatial diversity cab be obtained which leads to high resolution detection and localization [3]–[8]**.** The detection capability of MIMO radar and phased array radar, which typically has antenna separation of $d < \lambda/2$, have been compared in [3]. In addition, non-orthogonal signalling for MIMO radars is proposed in [4]. The effect of system impairments such as interference, fluctuating targets and synchronization errors are investigated in [9]–[11]. The relative information, or Kullback-Leibler divergence theorem has been adopted in [12]–[14] to analyze and design MIMO radars.

The integration between radar and communication (RadCom) systems has been recently proposed in the literature, and has attracted the research community. In RadCom systems, the resources of the base-station (BS) are utilized for both sensing and communications [15], [16]. In addition, RadCom systems can be very beneficial for sensing assisted communications such as channel estimation and spectrum sensing for cognitive radio networks [21], [22]. The performance of integrated sensing and communication (ISAC) system is analyzed in [17] using the communication user's rate and radar detection probability. In [18] and [19], ISAC systems are considered with uplink and downlink data transmissions, and the analysis are provided using the outage probability, ergodic communication rate and diversity order for the communication users, whereas the sensing rate is evaluated for the radar system. Besides, the probability of detection for the radar sensing part and the spectral efficiency for communication system are analyzed for a full-duplex ISAC system in [20], [23].

Obviously, RadCom systems are expected to play a pivotal role in future wireless networks. As can be depicted from the literature, the performance of RadCom systems is typically evaluated using different metrics, for example, the bit error rate for the communications and the detection probability for the sensing system. However, introducing a unified performance measure for both systems should be very useful especially when optimizing the available network resources. Consequently, the main objective of this work is to provide a unified performance measure applicable for measuring the performance of communication and radar subsystems at the same time using the Kullback-Leibler divergence theorem, also known as the relative information (RE). It is worth mentioning that although the RE theorem has been widely used to analyze and design radar systems, to the best of authors knowledge, it has not been considered to evaluate the MIMO communication systems. Moreover, we will show that RE can capture the detection performance for both systems by relating it to the symbol error rate (SER) of the communication system and the detection probability of the radar system [24], [25]. The obtained results show that derivations in this paper are very accurate and the proposed RE is informative about the RadCom system holistically.

Sec. II presents the system model. In Secs. III and IV, the analysis based Kullback-Leibler divergence (KLD) is provided for the communication and radar subsystems, respectively. Sec. V shows numerical results for the considered model, and finally a conclusion is provided in Sec. VI.

II. SYSTEM MODEL

The system model in this paper includes N antenna MIMO-BS serving a number of K communication user equipments (UEs) using $N_C < N$ antennas in downlink and aims at detecting an unmanned aerial vehicles (UAV) target using the remaining $N_R = N - N_C$ antennas. As shown in 1, the

M. Al-Jarrah and E. Alsusa are with the Department of Electrical and Electronic Engineering, University of Manchester, Manchester M13 9PL, U.K. (e-mail: {mohammad.al-jarrah, e.alsusa}@manchester.ac.uk).

C. Masouros is with the Department of Electronic and Electrical En gineering, University College London, London WC1E 7JE, U.K. (e-mail:chris.masouros@ieee.org).

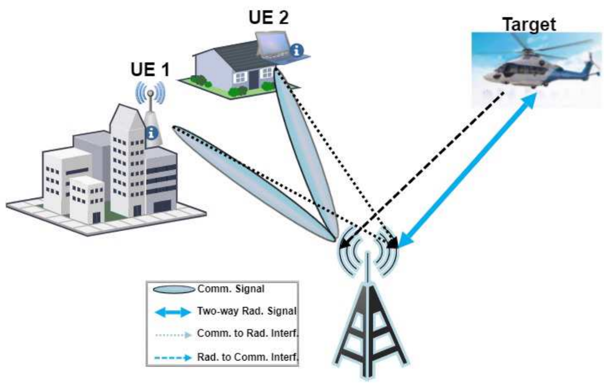

Fig. 1. An ISAC system with 2 UEs and 2 targets.

separated deployment, in which the BS antennas are divided between the communication and radar systems, is assumed. BS employs zero forcing (ZF) or maximum ratio transmission (MRT) to precode the UEs data information [26], [27]. The radar waveform matrix $\mathbf{S} = [\mathbf{s}_1, \mathbf{s}_2, \cdots, \mathbf{s}_L]$, where L is the number of snapshots and $\mathbf{s}_1 \in \mathbb{C}^{N_R \times 1}$ is the transmitted signals vector in the lth snapshot, is designed such that the resulting covariance matrix $\mathbf{R}_s \triangleq \frac{1}{L}\sum_{l=1}^{L}\mathbf{s}_l\mathbf{s}_l^H$ satisfies a desired form. The total amount of power available at BS, P_T, is also distributed among the communication and radar subsystems with P_C and $P_{\text{rad}} = P_T - P_C$, respectively.

For transmission interval l, a data symbol $d_k[l]$ intended for the kth UE is picked from a normalized M-ary phase shift keying (MPSK), i.e., $|d_k[l]|^2 = 1$, and precoded using a linear precoder with a precoding vector $\mathbf{w}_k \in \mathbb{C}^{N_C \times 1}$, and thus the precoded information symbols for all users can be written as

$$\mathbf{d}_{\mathbf{w}}[l] = \sum_{i=1}^{K} \sqrt{p_k}\mathbf{w}_k d_k[l] \tag{1}$$

where $p_k \forall k$ is a power control factor. Consequently, the received signal at the kth UE with a radar interference

$$y_k[l] = \mathbf{g}_k^T \mathbf{d}_{\mathbf{w}}[l] + \eta_k \tag{2}$$

where P_{rad} is the power allocated to the radar subsystem, $\mathbf{g}_k \in \mathbb{C}^{N_C \times 1} \sim \mathcal{CN}\left(0, 2\sigma_g^2\right)$ is a flat Rayleigh channel gain vector from the communication antennas to UE k, $\eta_k \triangleq \sqrt{\frac{P_{\text{rad}}}{N_R}}\mathbf{f}_k^T\mathbf{s}_l + n_k$ is the radar interference plus noise, $\mathbf{f}_k^T \in \mathbb{C}^{N_R \times 1} \sim \mathcal{CN}\left(0, 2\sigma_f^2\right)$ is a flat Rayleigh channel gain vector which represents the channel from the radar antennas to UEs, and $n_k \sim \mathcal{CN}\left(0, 2\sigma_n^2\right)$ is the additive white Gaussian noise (AWGN). It can be shown that $\eta_k \sim \mathcal{CN}\left(0, 2\sigma_\eta^2\right)$ where $\sigma_\eta^2 = \frac{P_{\text{rad}}}{N_R}\sigma_f^2 + \sigma_n^2$. It worth noting that in case of massive MIMO-BS, the radar signal can be designed such that the radar signal $\mathbf{s}_l$ falls into the null space of $\mathbf{f}_k^T$, i.e., $\mathbf{f}_k^T\mathbb{E}\left[\mathbf{s}_l\mathbf{s}_l^H\right]\mathbf{f}_k^* = 0$, which cancels the radar interference at UEs [15].

On the other hand, let the desired radar waveform $\mathbf{s}_l \in \mathbb{C}^{N_R \times 1} \forall l \leq L$, where L is the number of snapshots, and $\mathbf{a}_{\text{T}}(\theta)$ and $\mathbf{a}_{\text{R}}(\theta)$ are respectively the transmit and receive array manifold of a uniform linear array (ULA). Therefore, the received signals vector at BS can be expressed as a binary hypothesis testing problem

$$\tilde{\mathbf{y}}_{\text{rad}}[l] = \begin{cases} H_1 : \alpha\sqrt{\frac{P_{\text{rad}}}{N_R}}\mathbf{a}_{\text{R}}(\theta)\,\mathbf{a}_{\text{T}}(\theta)^T\mathbf{s}_l + \mathbf{G}_{\text{rad}}\mathbf{d}_{\mathbf{w}}[l] + \mathbf{n}_{\text{rad}}[l] \\ H_0 : \mathbf{G}_{\text{rad}}\mathbf{d}_{\mathbf{w}}[l] + \mathbf{n}_{\text{rad}}[l] \end{cases} \tag{3}$$

where H_0 and H_1 denote the absence and existence of a target, respectively, α is the channel gain for BS-Target-BS path, the term $\mathbf{G}_{\text{rad}}\mathbf{d}_{\mathbf{w}}[l]$ represents the interference caused by the communication signal, $\mathbf{G}_{\text{rad}}^T \in \mathbb{C}^{N_R \times N_C}$ is the channel matrix from the communication antennas to the radar antennas, and $\mathbf{n}_{\text{rad}} \in \mathbb{C}^{N_R \times 1} \sim \mathcal{CN}\left(0, 2\sigma_n^2\mathbf{I}_{N_R}\right)$ is the AWGN with $\mathbf{I}_{N_R}$ is the identity matrix. We assume that the channel side information (CSI) of $\mathbf{G}_{\text{rad}}$ is available at BS, and thus $\mathbf{G}_{\text{rad}}\mathbf{d}_{\mathbf{w}}[l]$ can be subtracted from $\tilde{\mathbf{y}}_{\text{rad}}[l]$. It is worth noting that the estimation of $\mathbf{G}_{\text{rad}}$ can be performed at the BS in a previous phase. Therefore, given the estimated channel matrix $\hat{\mathbf{G}}_{\text{rad}}$, the received signals in (3) after subtracting $\mathbf{G}_{\text{rad}}\mathbf{d}_{\mathbf{w}}[l]$ can be rewritten as

$$\mathbf{y}_{\text{rad}}[l] = \begin{cases} H_1 : \alpha\sqrt{\frac{P_{\text{rad}}}{N_R}}\mathbf{A}(\theta)\,\mathbf{s}_l + \boldsymbol{\omega}_{\text{rad}} + \mathbf{n}_{\text{rad}}[l] \\ H_0 : \boldsymbol{\omega}_{\text{rad}} + \mathbf{n}_{\text{rad}}[l] \end{cases} \tag{4}$$

where a monostatic radar is considered with $\mathbf{a}(\theta) \triangleq \mathbf{a}_{\text{R}}(\theta) = \mathbf{a}_{\text{T}}(\theta) \triangleq \left[1, \mathrm{e}^{j\frac{2\pi\Delta}{\lambda_0}\sin(\theta)}, \cdots, \mathrm{e}^{j\frac{2\pi\Delta}{\lambda_0}(N_R-1)\sin(\theta)}\right]^T$, $\mathbf{A}(\theta) \in \mathbb{C}^{N_R \times N_R} = \mathbf{a}(\theta)\,\mathbf{a}(\theta)^T$ is the equivalent array manifold, and $\boldsymbol{\omega}_{\text{rad}} \in \mathbb{C}^{N_R \times 1} = \mathbf{G}_{\text{err}}^T\mathbf{d}_{\mathbf{w}}[l] = \mathbf{G}_{\text{err}}^T\sum_{i=1}^{K}\sqrt{p_k}\mathbf{w}_k d_k[l]$ is the remaining communication signal interference after the subtraction process mentioned above, and $\mathbf{G}_{\text{err}} \triangleq \mathbf{G}_{\text{rad}} - \hat{\mathbf{G}}_{\text{rad}}$ representing channel estimation errors. In this paper, we consider imperfect channel estimation, and the estimation error is modeled as a complex Gaussian random variable with a mean of 0 and a variance of σ_{err}^2.

III. The Relative Entropy of Communication System

In this section, KLD will be evaluated for the communication subsystem where ZF and MRT precoders are considered with long-term matrix power normalization.

For a pair continuous probability density functions, $f_m(x)$ and $f_n(x)$, $\text{KLD}_{n\to m}$ is defined as the relative entropy from $f_n(x)$ to $f_m(x)$ or a measure of how different a PDF $f_n(x)$ is from another PDF $f_m(x)$. In general , KLD is asymmetric metric, and mathematically $\text{KLD}_{n\to m}$ for continuous random variables can be represented as

$$\text{KLD}(f_m \parallel f_n) = \int_{-\infty}^{\infty} f_n(x)\log_2\left(\frac{f_n(x)}{f_m(x)}\right)dx, \tag{5}$$

and for multivariate Gaussian distributed random variables having mean vectors of $\boldsymbol{\mu}_m$ and $\boldsymbol{\mu}_n$ and covariance matrices of Σ_m and Σ_n, it can be derived as

$$\begin{aligned}\text{KLD}_{n\to m} = \frac{1}{2\ln 2}\Big(&\text{tr}\left(\Sigma_n^{-1}\Sigma_m\right) - 2 + \ln\frac{|\Sigma_n|}{|\Sigma_m|} \\ &+ \left(\boldsymbol{\mu}_{k,n} - \boldsymbol{\mu}_{k,m}\right)^T\Sigma_n^{-1}\left(\boldsymbol{\mu}_{k,n} - \boldsymbol{\mu}_{k,m}\right)\Big)\end{aligned} \tag{6}$$

A. ZF based Data Precoding

Here, we assume ZF is employed at BS, which is able to cancel out the interference between users. The precoding matrix $\mathbf{W}$ for ZF case is generally given by $\mathbf{W} = \mathbf{P}\mathbf{G}^H \left(\mathbf{G}\mathbf{G}^H\right)^{-1}$, where $\mathbf{P}$ is a diagonal matrix used to control the transmit power of each UE. Consequently, the received signals vector at UEs can be written as

$$\mathbf{y}[l] = \mathbf{P}\mathbf{d} + \boldsymbol{\eta} \tag{7}$$

where $\mathbf{P}$ is

$$\mathbf{P} \triangleq \alpha_{\mathrm{ZF}} \mathbf{P}_{\mathrm{com}} = \sqrt{N_C - K + 1}\,\mathbf{P}_{\mathrm{com}} \tag{8}$$

where $\alpha_{\mathrm{ZF}} = \sqrt{N_C - K + 1}$ is a normalization factor to ensure that the average transmit power is fixed and $\mathbf{P}_{\mathrm{com}} \triangleq \mathrm{diag}\left(\sqrt{P_{1,\mathrm{com}}}, \sqrt{P_{2,\mathrm{com}}}, \cdots, \sqrt{P_{K,\mathrm{com}}}\right)$ is used to control the amount of power for each UE. The total amount of power is limited to P_C, $\sum_k P_{k,\mathrm{com}} = P_C$ [27], and it can be selected such that $P_{k,\mathrm{com}} = \frac{P_C}{K}$ for uniform power allocation among UEs. The received signal at the kth user can be rewritten as

$$y_k[l] = \sqrt{P_{k,\mathrm{com}}}\,\alpha_{\mathrm{ZF}} d_k[l] + \eta_k \tag{9}$$

Based on the received signal $y_k[l]$, the conditional probability density function $f(y_k|d_k[l])$ is complex Gaussian and can be written as

$$f(y_k|d_k[l]) = \frac{1}{\sqrt{(2\pi)^2 |\Sigma|}} \mathrm{e}^{-(\mathbf{y}_k - \boldsymbol{\mu}_k)^T \Sigma^{-1} (\mathbf{y}_k - \boldsymbol{\mu}_k)} \tag{10}$$

where $\mathbf{y}_k \triangleq [y_{k,\Re}, y_{k,\Im}]^T$ with $y_{k,\Re} \triangleq \mathrm{Re}(y_k)$ and $y_{k,\Im} = \mathrm{Im}(y_k)$ denote the real and imaginary components of y_k, respectively, $\boldsymbol{\mu}_k \triangleq [\mu_{k,\Re}, \mu_{k,\Im}]^T$ with $\mu_{k,\Re} = \sqrt{P_{k,\mathrm{com}}}\alpha_{\mathrm{ZF}} \mathrm{Re}(d_k[l])$ and $\mu_{k,\Im} = \sqrt{P_{k,\mathrm{com}}}\alpha_{\mathrm{ZF}} \mathrm{Im}(d_k[l])$, $\Sigma = \sigma_\eta^2 \mathbf{I}_2$, and $|\Sigma| = \sigma_\eta^4$ and $\Sigma^{-1} = \frac{1}{\sigma_\eta^2}\mathbf{I}_2$.

For MPSK, KLD should be evaluated for each possible pair of unequal data symbols $\{d_{k,n}[l], d_{k,m}[l]\}$. Let us consider a pair of MPSK symbols, $\{d_{k,n}[l], d_{k,m}[l]\}\,\forall n \neq m$, with density functions given by $f_n \sim \mathcal{CN}(\boldsymbol{\mu}_{k,n}, \Sigma_n)$ and $f_m \sim \mathcal{CN}(\boldsymbol{\mu}_{k,n}, \Sigma_m)$, thus $\mathrm{KLD}_{n\to m}$ can be derived as,

$$\begin{aligned}\mathrm{KLD}_{k,n\to m} = \frac{1}{2\ln 2}\Bigg(&\mathrm{tr}\left(\Sigma_m^{-1}\Sigma_n\right) - 2 + \ln\frac{|\Sigma_m|}{|\Sigma_n|} \\ &+ (\boldsymbol{\mu}_{k,m} - \boldsymbol{\mu}_{k,n})^H \Sigma_m^{-1} (\boldsymbol{\mu}_{k,m} - \boldsymbol{\mu}_{k,n})\Bigg)\end{aligned} \tag{11}$$

Moreover, by noting that $\Sigma_n = \Sigma_m = \sigma_\eta^2 \mathbf{I}_2$, and given that $\boldsymbol{\mu}_{k,m} = \left[\sqrt{P_{k,\mathrm{com}}}\alpha_{\mathrm{ZF}} \cos\phi_{k,m}, \sqrt{P_{k,\mathrm{com}}}\alpha_{\mathrm{ZF}} \sin\phi_{k,m}\right]$, $\mathrm{KLD}_{n\to m}$ for long-term normalization based ZF can be simplified to

$$\begin{aligned}\mathrm{KLD}_{k,n\to m}^{\mathrm{ZF}} &= \frac{1}{2\sigma_\eta^2 \ln 2} (\boldsymbol{\mu}_{k,m} - \boldsymbol{\mu}_{k,n})^H (\boldsymbol{\mu}_{k,m} - \boldsymbol{\mu}_{k,n}) \\ &= \frac{\gamma_{k,\mathrm{ZF}}}{\ln 2}\left(1 - \cos\left(\phi_{k,m} - \phi_{k,n}\right)\right)\end{aligned} \tag{12}$$

where $\gamma_{k,\mathrm{ZF}} = \frac{\alpha_{\mathrm{ZF}}^2 P_{k,\mathrm{com}}}{\sigma_\eta^2}$.

As stated earlier, since KLD is measured for a pair of PDFs, the average KLD, $\mathrm{KLD}_{k,\mathrm{avg}}^{\mathrm{ZF}}$, should be evaluated by considering all possible pairs of dissimilar symbols, which can be represented as

$$\begin{aligned}\mathrm{KLD}_{k,\mathrm{avg}}^{\mathrm{ZF}} &= \frac{\gamma_{\mathrm{LTZF}}}{\ln 2}\sum_{m=1}^{M}\sum_{\substack{n=1\\n\neq m}}^{M} \Pr\left(\phi_{k,m}, \phi_{k,n}\right)\left(1 - \cos\left(\phi_{k,m} - \phi_{k,n}\right)\right) \\ &= \frac{\lambda}{M(M-1)\ln 2}\gamma_{\mathrm{LTZF}}\end{aligned} \tag{13}$$

where $\lambda = \sum_{m=1}^{M}\sum_{\substack{n=1\\n\neq m}}^{M}\left(1 - \cos\left(\phi_{k,m} - \phi_{k,n}\right)\right)$. Finally, the average KLD value for all UEs can be expressed as

$$\mathrm{KLD}_{\mathrm{ZF}} = \frac{1}{K}\sum_{k=1}^{K}\mathrm{KLD}_{k,\mathrm{avg}}^{\mathrm{ZF}} \tag{14}$$

B. MRT based Data Precoding

The MRT precoding vector for the kth user data, $\mathbf{w}_k$, is evaluated based on the channel vector $\mathbf{h}_k$ as $\mathbf{w}_k = \sqrt{\frac{P_{k,\mathrm{com}}}{\mathbb{E}\left[\mathbf{g}_k \mathbf{g}_k^H\right]}}\mathbf{g}_k^H$, where $\mathbb{E}\left[\mathbf{g}_k \mathbf{g}_k^H\right] = 2N_C\sigma_g^2$ and the received signal at the kth UE is

$$\begin{aligned}y_k[l] &= \mathbf{g}_k^T \sum_{k=1}^{K}\mathbf{w}_k d_k[l] + \eta_k \\ &= \sqrt{\frac{P_{k,\mathrm{com}}}{2N_C\sigma_g^2}}\|\mathbf{g}_k\|^2 d_k[l] + \omega_{\mathrm{MRT}}\end{aligned} \tag{15}$$

where $\omega_{\mathrm{MRT}} = \mathbf{g}_k^T \sum_{\substack{i=1\\i\neq k}}^{K}\sqrt{\frac{P_{i,\mathrm{com}}}{2N_C\sigma_g^2}}\mathbf{g}_i^H d_i[l] + \eta_k$ represents the radar and communication interference plus noise. Given that $\mathbf{g}_k$ and $\mathbf{g}_i^T \forall i \neq k$ are independent identically distributed (i.i.d) with 0 mean and $\eta_k \sim \mathcal{CN}(0, 2\sigma_\eta^2)$, the central limit theorem (CLT) can be employed to asymptotically find the density of ω_{MRT}. Accordingly, ω_{MRT} can be seen as a complex Gaussian random variable with 0 mean and a variance of

$$\begin{aligned}\sigma_\omega^2 &= \mathrm{var}\left[\mathbf{g}_k^T \sum_{\substack{i=1\\i\neq k}}^{K}\sqrt{\frac{P_{i,\mathrm{com}}}{2N_C\sigma_g^2}}\mathbf{g}_i^H d_i[l] + \eta_k\right] \\ &= \sum_{n_c=1}^{N_C}\sum_{\substack{i=1\\i\neq k}}^{K}\sqrt{\frac{P_{i,\mathrm{com}}}{2N_C\sigma_g^2}}\mathrm{var}\left[\mathbf{g}_k^T(n_c)\,\mathbf{g}_i^H(n_c)\,d_i[l]\right] + \mathrm{var}[\eta_k]\end{aligned} \tag{16}$$

where $\mathbf{g}_k^T(n_c)$ is the element number n_c of the channel vector $\mathbf{g}_k^T$. Given that $|d_i[l]|^2 = 1$, as well as $\mathbf{g}_k^T$ and $\mathbf{g}_i^H$ are independent, σ_ω^2 can be then found as

$$\begin{aligned}\sigma_\omega^2 &= \sum_{n_c=1}^{N_C}\sum_{\substack{i=1\\i\neq k}}^{K}\sqrt{\frac{P_{i,\mathrm{com}}}{2N_C\sigma_g^2}}\mathrm{var}\left[\mathbf{g}_k^T(n_c)\right]\mathrm{var}\left[\mathbf{g}_i^H(n_c)\right] + \mathrm{var}[\eta_k] \\ &= 2\sqrt{2N_C}\sigma_g^3 \sum_{\substack{i=1\\i\neq k}}^{K}\sqrt{P_{i,\mathrm{com}}} + 2\sigma_\eta^2\end{aligned} \tag{17}$$

Consequently, following the definition of KLD in (6), the relative entropy for MRT scenario can be found as

$$\mathrm{KLD}_{k,\mathrm{MRT,avg}} = \frac{\lambda}{M(M-1)\ln 2}\frac{P_{k,\mathrm{com}}}{2N_C\sigma_g^2\sigma_\omega^2}\mathbb{E}\left[\|\mathbf{g}_k\|^4\right] \tag{18}$$

Given that $|\mathbf{g}_k(n_c)|$ is Rayleigh distributed with a scale parameter σ_g, i.e., $|\mathbf{g}_k(n_c)| \sim \text{Rayleigh}(\sigma_g)$, therefore, $\|\mathbf{g}_k\|^2 = \sum_{n_c=1}^{N_C} |\mathbf{g}_k(n_c)|^2$ has Gamma distribution with shape and scale parameters of N_C and $2\sigma_g^2$, respectively, i.e., $\|\mathbf{g}_k\|^2 \sim \text{Gamma}\left(N_C, 2\sigma_g^2\right)$. Consequently, the average relative entropy for the kth UE is

$$\text{KLD}_{k,\text{MRT},\text{avg}} = \frac{2\sigma_g^2 \lambda}{M(M-1)\sigma_\omega^2 \ln 2}(1+N_C)P_{k,\text{com}} \quad (19)$$

Finally, the average KLD for all communication UEs can be then written as

$$\text{KLD}_{\text{MRT}} = \frac{1}{K}\sum_{k=1}^{K}\text{KLD}_{k,\text{MRT},\text{avg}} \quad (20)$$

IV. The Relative Entropy of Radar System

Based on (4) and assuming that the error caused by imperfect IC scheme is complex Gaussian $\boldsymbol{\omega}_{\text{rad}} \sim \mathcal{CN}\left(0, 2\sigma_\omega^2 \mathbf{I}_{N_R}\right)$, the received radar signals can be expressed as

$$\mathbf{y}_{\text{rad}}[l] = \begin{cases} H_1 : \alpha\sqrt{\frac{P_{\text{rad}}}{N_R}}\mathbf{A}(\theta)\mathbf{s}_l + \tilde{\boldsymbol{\omega}}_{\text{rad}} \\ H_0 : \tilde{\boldsymbol{\omega}}_{\text{rad}} \end{cases} \quad (21)$$

where $\tilde{\boldsymbol{\omega}}_{\text{rad}} \sim \mathcal{CN}\left(0, 2\sigma_{\tilde{\omega}}^2 \mathbf{I}_{N_R}\right)$ with $\sigma_{\tilde{\omega}}^2 = \sigma_\omega^2 + \sigma_n^2$ and $\sigma_\omega^2 = \sigma_{\text{err}}^2 \sigma_{\text{w}}^2 N_C \sum_{i=1}^{K} P_{k,\text{com}}$. The sufficient statistics of the generalized likelihood ratio test, denoted as $\xi(\theta_k)$, is asymptotically Chi-squared distributed with the following statistics [3], [4], [8], [9], [28],

$$\xi(\theta_k) \sim \begin{cases} H_1 : \mathcal{X}_2^2(\lambda) \\ H_0 : \mathcal{X}_2^2(0) \end{cases} \quad (22)$$

where $\mathcal{X}_2^2$ denotes noncentral Chi-squared random variable with 2 degrees of freedom and $\lambda_{\text{rad}} = \frac{|\alpha|^2}{\sigma_{\tilde{\omega}}^2}\frac{P_{\text{rad}}}{N_R}\left|\mathbf{a}^H(\theta)\mathbf{R}_s\mathbf{a}(\theta)\right|^2$ is the noncentrality parameter of $\xi(\theta_k)$ under hypothesis H_1. By using the definition of KLD, the KLD from ξ_{H_1} to ξ_{H_0} in this case can be derived as

$$\text{KLD}_{H_{1\to 0}} = \int_{-\infty}^{\infty} f_\xi(\xi|H_0)\log_2\left(\frac{f_\xi(\xi|H_0)}{f_\xi(\xi|H_1)}\right)d\xi \quad (23)$$

After substituting $f_\xi(\xi|H_0)$ and $f_\xi(\xi|H_1)$,

$$\text{KLD}_{H_{1\to 0}} = \frac{\lambda \log_2 \text{e}}{4}\int_0^\infty \text{e}^{-0.5\xi}d\xi - \frac{1}{2}\int_0^\infty \text{e}^{-0.5\xi}\log_2\left(I_0\left(\sqrt{\lambda\xi}\right)\right)d\xi, \quad (24)$$

which can be simplified to

$$\text{KLD}_{H_{1\to 0}} = \frac{1}{2}\left(1.4427\lambda - \frac{1}{\ln 2}\int_0^\infty \text{e}^{-0.5\xi}\ln\left(I_0\left(\sqrt{\lambda\xi}\right)\right)\right)d\xi \quad (25)$$

By using Maple, it can be observed that the limit of the integrand is 0 as $\xi \to \infty$. Consequently, we solve this integral numerically by using trapezoidal method due to the space limit. Similarly, $\text{KLD}_{H_{0\to 1}}$ can be found as

$$\text{KLD}_{H_{1\to 0}} = \int_{-\infty}^{\infty} f_\xi(\xi|H_1)\log_2\left(\frac{f_\xi(\xi|H_1)}{f_\xi(\xi|H_0)}\right)d\xi \quad (26)$$

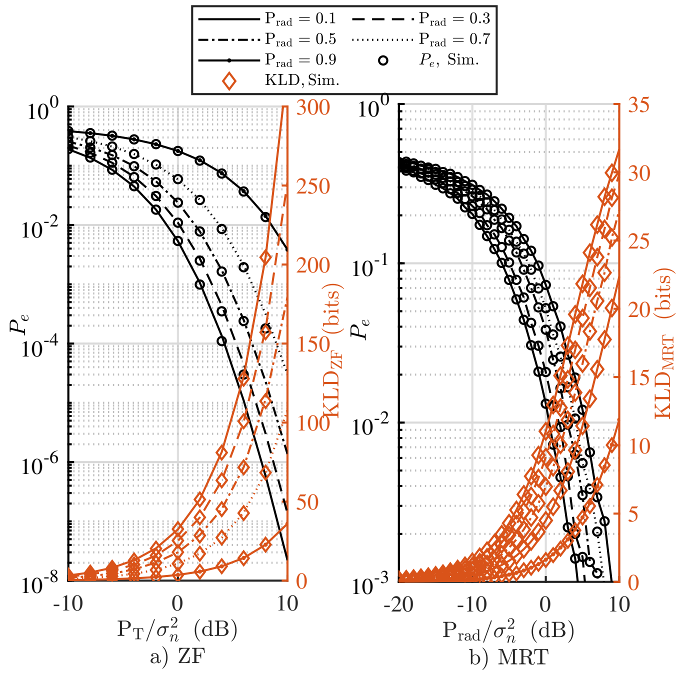

Fig. 2. The BER and KLD measure versus the transmit SNR P_T/σ_n^2 for both CUs with several values of P_{rad} and for a) ZF and b) MRT.

After substituting the corresponding density functions,

$$\text{KLD}_{H_{1\to 0}} = \frac{-0.5\lambda \text{e}^{-0.5\lambda}}{2\ln 2}\int_0^\infty \text{e}^{-0.5\xi}I_0\left(\sqrt{\lambda\xi}\right)d\xi + \frac{\text{e}^{-0.5\lambda}}{2\ln 2}\int_0^\infty \text{e}^{-0.5\xi}I_0\left(\sqrt{\lambda\xi}\right)\ln\left(I_0\left(\sqrt{\lambda\xi}\right)\right)d\xi \quad (27)$$

By solving the first integral using [29], $\text{KLD}_{H_{1\to 0}}$ can be simplified to

$$\text{KLD}_{H_{1\to 0}} = \frac{-0.5\lambda}{\ln 2} + \frac{\text{e}^{-0.5\lambda}}{2\ln 2}\mathcal{I}_3 \quad (28)$$

where $\mathcal{I}_3 = \int_0^\infty \text{e}^{-0.5\xi}I_0\left(\sqrt{\lambda\xi}\right)\ln\left(I_0\left(\sqrt{\lambda\xi}\right)\right)d\xi$, which is solved using trapezoidal numerical integration method. Finally, KLD is evaluated based on the average value of $\text{KLD}_{H_{1\to 0}}$ and $\text{KLD}_{H_{0\to 1}}$, which for equal probable H_0 and H_1, i.e., $\Pr(H_0) = \Pr(H_1) = 0.5$, can be written as

$$\text{KLD}_{\text{rad}} = \frac{1}{2}\left(\text{KLD}_{H_{0\to 1}} + \text{KLD}_{H_{1\to 0}}\right) \quad (29)$$

V. Numerical Results

The section presents the measured performance of the ISAC system introduced in this paper. Monte Carlo simulation with 10^6 realizations for each run is used to generate the simulation (Sim.) results and the derived formulas in this paper are used to generate the theoretical performance. Two UEs and a single target scenario have been considered with $L = 100$ snapshots and antenna separation of half the wavelength, $\Delta = 0.5\lambda$. Moreover, the total transmit power is normalized to $P_T = 1$, the target is located at $\theta = 35^o$, the radar covariance matrix is designed such that $\mathbf{R}_s = \mathbf{I}_{N_R}$, and the radar channel pathloss is normalized, $\alpha = 1$.

Figs. 2 and 3 present the measured theoretical and simulated performance an ISAC system which consists of a 20 antenna BS serving 2 UEs through ZF (Fig. 2a) and MRT (Fig. 2b) precoding with BPSK signalling, and aiming at detecting the target. For these figures, each subsystem is allocated 10 antennas, the radar signal is well designed such that it does not cause interference with the communication signal received by UEs, i.e., $\mathbf{f}_k^T \mathbb{E}\left[\mathbf{s}_l \mathbf{s}_l^H\right] \mathbf{f}_k^* = 0$, as well as, $\mathbf{G}_{\mathrm{rad}}$ is perfectly estimated at BS, i.e., $\boldsymbol{\omega}_{\mathrm{rad}} \to 0$. As can be observed from these figures, the derived equations for the radar and communication KLDs match the simulation results. In addition, Figs. 2a and 2b show that the KLD of the communication system is inversely proportional to P_e, whereas it is directly proportional to the detection probability of the radar subsystem, P_{D}, as can be realized by comparing Fig. 3a and Fig. 3b. Moreover, increasing P_{rad} would enhance the detection capability of the radar system through increasing KLD and P_{D}; however, as the total transmission power is fixed, the portion allocated to the communication system decreases resulting in a higher error rate.

Fig. 4 presents the impact of interference caused from radar subsystem to UEs and the effect of estimation errors in $\mathbf{G}_{\mathrm{rad}}$. The total number of BS antennas is 20 with 10 antennas are assigned for each subsystem and QPSK signalling is employed for the communication subsystem. A number of 2 UEs and 100 snapshots are assumed and the power allocated for radar and communication are respectively $P_{\mathrm{R}} = 0.1$ and $P_{\mathrm{C}} = 0.9$. As can be observed from the figure, the simulation results confirm the accuracy of the derived equations in this paper for $\mathrm{KLD}_{\mathrm{rad}}$, $\mathrm{KLD}_{\mathrm{ZF}}$ and $\mathrm{KLD}_{\mathrm{MRT}}$. It can be also seen that the interference caused by one subsystem to the other has sever impact and can limit the performance of the whole system. For example, for the case of ZF precoding, Fig. 4a shows that the probability of error for UEs suffers from an error floor at about 5×10^{-6}, and $\mathrm{KLD}_{\mathrm{ZF}}$ also reaches an upper bound of about 54 bits for $\frac{P_{\mathrm{T}}}{\sigma_n^2} \gtrsim 30$ dB. Moreover, MRT precoding suffers from relatively very bad performance which can be attributed to the fact that a certain UE suffers from inter-user interference in addition to radar signal interference. It can be also seen from 4b and 4c that the impact of channel estimation errors in $\mathbf{G}_{\mathrm{rad}}$ is very severe at considerable values of σ_{err}^2. For instance, a very low detection probability of about 0.2 is obtained when $\sigma_{\mathrm{err}}^2 = 0.1$ even at very high SNRs, and a KLD of about 3.45 bits is achieved for the same values of σ_{err}^2.

VI. Conclusion

A RadCom system which consists of a single BS serving a number of UEs sensing a target was introduced in this paper, where the separated deployment was considered. ZF and MRT precoders were employed to multiplex multiple data symbols intended for UEs. The relative entropy or KLD was derived for both radar and communication subsystems. Moreover, the effect of interference caused by the radar subsystem on UEs and the effect of imperfect interference cancellation on the radar subsystem were studied. The derived KLD was emphasized by Monti Carlo simulations. The results showed that there is a trade-off between the radar and communication subsystems where enhancing the detection capability of one negatively affects the other as the amount of interference increases accordingly.

Acknowledgment

This project has received funding from the European Union's Horizon 2020 research and innovation program under grant agreement No 812991.

References

[1] M. A. Al-Jarrah, M. A. Yaseen, A. Al-Dweik, O. A. Dobre and E. Alsusa, "Decision fusion for IoT-based wireless sensor networks," *IEEE IoT J.*, vol. 7, no. 2, pp. 1313-1326, Feb. 2020.

[2] M. Al-Jarrah, N. Al-Ababneh, M. Al-Ibrahim, R. Al-Jarrah, "Cooperative OFDM for semi distributed detection in wireless sensor networks," *AEU-Int. J. Electron. Commun.*, vol. 68, no. 10, pp. 1022-1029, 2014.

[3] E. Fishler, A. Haimovich, R. Blum, L. Cimini, D. Chizhik, and R. Valenzuela, "Spatial diversity in radars—Models and detection performance," *IEEE Trans. Signal Process.*, vol. 54, no. 3, pp. 823-838, Mar. 2006.

[4] I. Bekkerman and J. Tabrikian, "Target detection and localization using MIMO radars and sonars," *IEEE Trans. Signal Process.*, vol. 54, no. 10, pp. 3873-3883, Oct. 2006.

[5] A. Hassanien and S. Vorobyov, "Phased-MIMO radar: A tradeoff between phased-array and MIMO radars," *IEEE Trans.Signal Process.*, vol. 58, no. 6, pp. 3137-3151, Jun. 2010, doi: 10.1109/TSP.2010.2043976.

[6] H. Godrich, A. Haimovich, and R. Blum, "Target localization accuracy gain in MIMO radar-based systems," *IEEE Trans. Inf. Theory*, vol. 56, no. 6, pp. 2783-2803, June 2010, doi: 10.1109/TIT.2010.2046246.

[7] S. Ahmed and M. Alouini, "MIMO radar transmit beampattern design without synthesising the covariance matrix," *IEEE Trans. Signal Process.*, vol. 62, no. 9, pp. 2278-2289, May 2014.

[8] B. Friedlander, "On transmit beamforming for MIMO radar," *IEEE Trans. Aerosp. Electron. Syst.*, vol. 48, no. 4, pp. 3376-3388, Oct. 2012.

[9] A. Khawar, A. Abdelhadi and C. Clancy, "Target detection performance of spectrum sharing MIMO radars," *IEEE Sensors J.*, vol. 15, no. 9, pp. 4928-4940, Sep. 2015.

[10] Y. Yang, S.-P. Xiao, X.-S. Wang, and Y.-Z. Li, "Non-coherent radar detection probability for correlated gamma fluctuating targets in K distributed clutter," *IEEE Access*, vol. 6, pp. 3824-3827, 2018, doi: 10.1109/ACCESS.2017.2783878.

[11] J. Zuk, "Correlated noncoherent radar detection for gamma-fluctuating targets in compound clutter," *IEEE Trans. Aerosp. Electron. Syst*, vol. 58, no. 2, pp. 1241-1256, Apr. 2022.

[12] B. Tang, J. Tang, and Y. Peng, "MIMO radar waveform design in colored noise based on information theory," *IEEE Trans. Signal Process.*, vol. 58, no. 9, pp. 4684-4697, Sep. 2010.

[13] E. Grossi and M. Lops, "Kullback-Leibler divergence region in MIMO radar detection problems," *2012 15th Int. Conf. Inf. Fusion*, Singapore, 2012, pp. 896-901.

[14] L. Wang, K.-K. Wong, H. Wang, Y. Qin, "MIMO radar adaptive waveform design for extended target recognition," *Int. J. Distrib. Sensor Netw.*, Jun. 2015.

[15] F. Liu, C. Masouros, A. Li, H. Sun, and L. Hanzo, "MU-MIMO communications with MIMO radar: From co-Existence to joint transmission," *IEEE Trans. Wireless Commun.*, vol. 17, no. 4, pp. 2755-2770, Apr. 2018.

[16] A. Liu *et al.*, "A survey on fundamental limits of integrated sensing and communication," *IEEE Commun. Surveys Tuts.*, Early access, 2022.

[17] B. Chalise, M. Amin, and B. Himed, "Performance tradeoff in a unified passive radar and communications system," *IEEE Signal Process. Lett.*, vol. 24, no. 9, pp. 1275-1279, Sep. 2017.

[18] C.-C. Ouyang, Y. Liu, and H. Yang, "Fundamental performance of integrated sensing and communications (ISAC) systems," *arXiv Preprint*, 2022, Online. [Available]: https://arxiv.org/abs/2202.06207.

[19] C.-C. Ouyang, Y. Liu, and H. Yang, "On the performance of uplink ISAC systems," *arXiv Preprint*, 2022, Online. [Available]: https://arxiv.org/abs/2201.01422.

[20] Z. Xiao and Y. Zeng, "Full-duplex integrated sensing and communication: Waveform design and performance analysis," *2021 13th Int. Con. Wireless Commun. Signal Process. (WCSP)*, Changsha, China, 2021, pp. 1-5, doi: 10.1109/WCSP52459.2021.9613663.

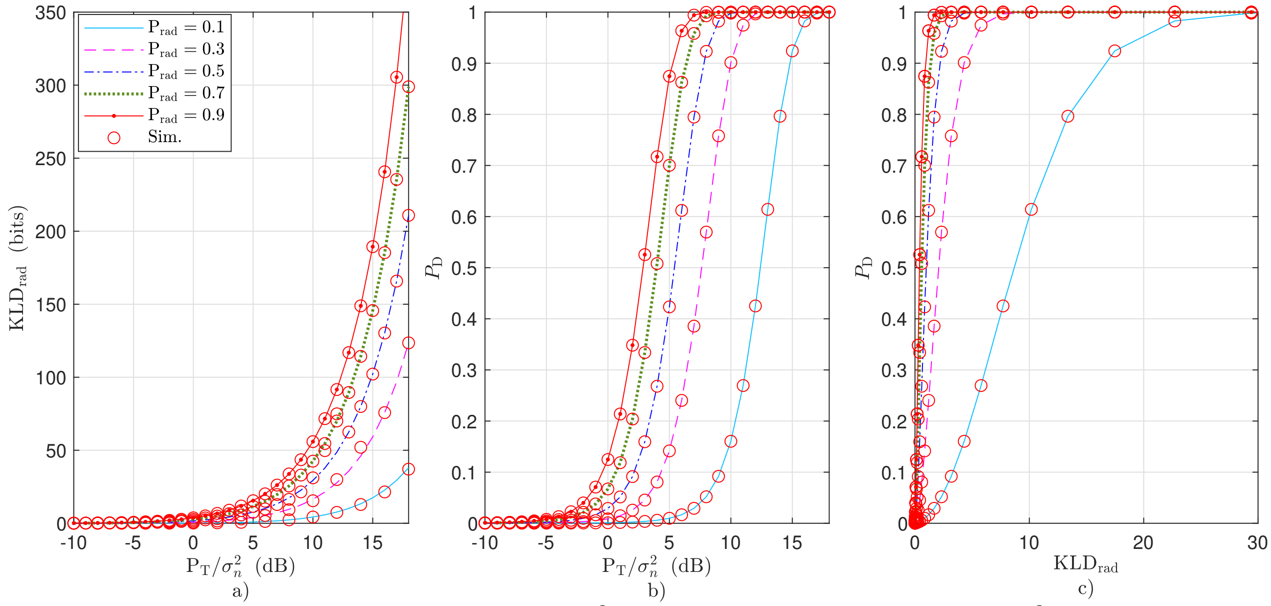

Fig. 3. The performance of radar subsystem versus the transmit SNR P_T/σ_n^2 for several values of P_{rad}: a) $\mathrm{KLD}_{\mathbf{rad}}$ vs. $P_{\mathrm{T}}/\sigma_n^2$, b) The detection probability P_{D} vs. $P_{\mathrm{T}}/\sigma_n^2$, and c) The detection probability P_{D} vs $\mathrm{KLD}_{\mathbf{rad}}$.

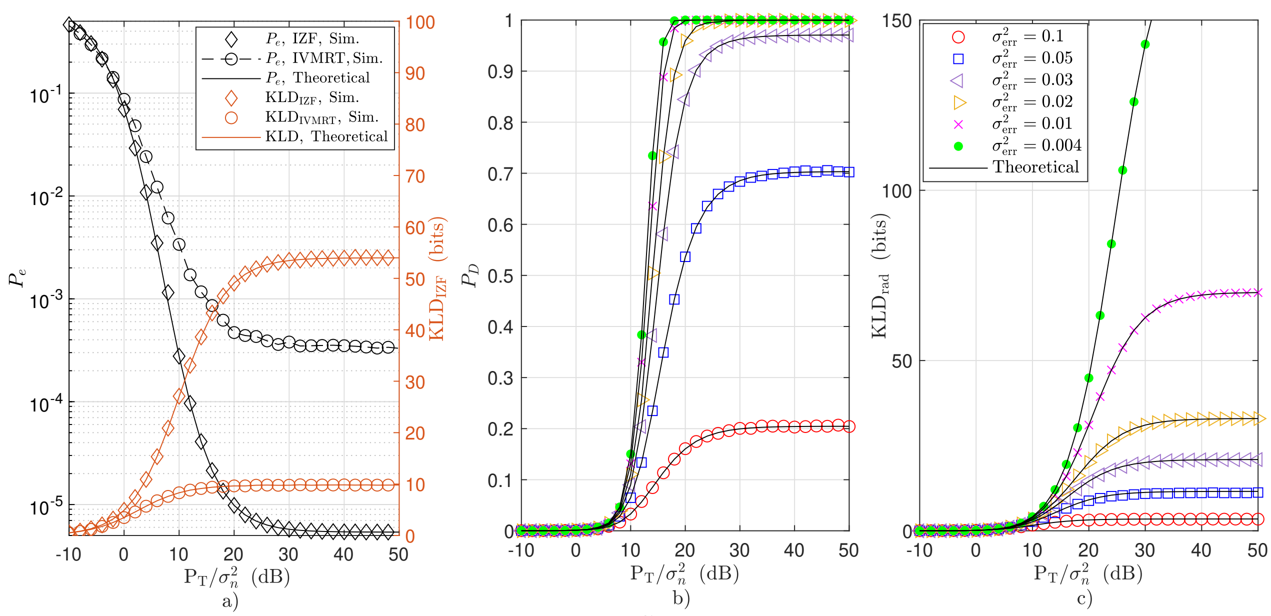

Fig. 4. The impact of radar-to-CUs interference and the estimation errors of $\mathbf{G}_{\mathbf{rad}}$ on the performance of CUs and radar subsystem, respectively, versus the transmit SNR P_T/σ_n^2: a) The error rate and KLD of CUs, b) The detection probability P_{D} for radar subsystem, and c) The KLD for the radar subsystems.

[21] F. Liu *et al*., "Integrated sensing and communications: Toward dual-functional wireless networks for 6G and beyond," *IEEE J. Sel. Areas Commun*., vol. 40, no. 6, pp. 1728-1767, Jun. 2022.

[22] M. A. Al-Jarrah, A. Al-Dweik, S. Ikki, and E. Alsusa, "Spectrum-occupancy aware cooperative spectrum sensing using adaptive detection," *IEEE Sys. J.*, vol. 14, no. 2, pp. 2225-2236, Jun. 2020.

[23] Z. Xiao and Y. Zeng, "Waveform design and performance analysis for full-duplex integrated sensing and communication," *IEEE J. Sel. Areas Commun.*, Early access, 2022, doi: 10.1109/JSAC.2022.3155509.

[24] T. M. Cover and J. A. Thomas, Elements of Information Theory. New York: Wiley, 1991.

[25] M. Al-Jarrah, R. Al-Jarrah, N. Al-Ababneh, "Decision fusion in mobile wireless sensor networks using cooperative multiple symbol differential space time coding", *AEU-Int. J. Electron. Commun.*, vol. 80, pp. 127-136, 2017.

[26] N. Fatema, G. Hua, Y. Xiang, D. Peng, and I. Natgunanathan, "Massive MIMO linear precoding: A survey," *IEEE Sys. J.*, vol. 12, no. 4, pp. 3920-3931, Dec. 2018, doi: 10.1109/JSYST.2017.2776401.

[27] A. Stavridis, M. Renzo, and H. Haas, "Performance analysis of multi-stream receive spatial modulation in the MIMO broadcast channel," *IEEE Trans. Wireless Commun*., vol. 15, no. 3, pp. 1808-1820, Mar. 2016.

[28] S. Kay, Fundementals of Statistical Signal Processing: Part II. Englewood Cliffs, NJ: Prentice-Hall, 1998.

[29] A. Prudnikov, Y. Brychkov, and O. Marichev, *Integrals Series: Special Functions*, 3rd ed. London, U.K.: Gordon and Breach Science Publishers, 1986.